Static Structural and Transient Dynamic Analysis of 6200 Deep Groove Ball Bearing

Putti Srinivasa Rao[#1], NariseSaralika[#2]

[#]*Department of Mechanical Engineering, Andhra University, Visakhapatnam, Andhra Pradesh, India.*

Abstract—*Parameters like stresses induced, deformations formed, and strains are very much important to analyze the failure mode of the deep groove ball bearing consisting of outer ring, inner ring, balls, and the cage. In the present work, 6200 deep groove ball Bearing is considered and four different materials are used for analysis. First bearing is made up of complete stainless steel; second and third Bearings are hybrid Bearings in which the inner and outer raceways are made up of stainless steel and the balls are made up of ceramic materials namely aluminum oxide and zirconium oxide respectively, and the fourth Bearing is a ceramic ball Bearing which is completely made up of aluminum oxide. Contact stresses, deformations, Von Mises-stresses, and strains are calculated both theoretically and by using ANSYS. The deep groove ball Bearing is modeled by using CATIA. Stresses, deformations and strains for varying applied loads are obtained from static structural analysis by using ANSYS. Both the theoretical and ANSYS results are in good agreement. The variation in the deformations and the stresses with respect to time due to impact loading are studied by using transient dynamic loading using ANSYS. The results obtained from transient dynamic analysis and the structural analysis are found to be nearly same.*

Keywords —*Deep groove ball bearings, Contact stresses, Deformations, CATIA, ANSYS, Von-Mises stresses, Transient Dynamic Analysis.*

I. INTRODUCTION

The primary goal of this work is obtain the Static Structural and transient dynamic analysis results and then compare the results to find best deep groove ball bearing among the four bearings considered. Hybrid and ceramic ball bearings are being recently studied upon due to their high strength bearing capacity and lower wear when compared to steel bearings. The contact finite element analysis can show bearings' information under contact, such as contact stress, strain, penetration and sliding distance, and so on, which play a significant role in optimum design of complicated rolling bearings [1]. Fatigue analysis to predict the minimum service life on bearing is carried out by various researchers and the load carrying capacity and corresponding service life are the important area of research to understand the component behavior [2].

The influence of housing deformation on load distribution in the bearing by two different approaches' a finite element approach and a semi-analytical approach where the rolling elements are replaced by user elements is studied [3]. The contact stress under different structural parameters are analyzed in detail and the changing laws of curvature coefficient, the number and diameter of the rolling element and contact stress are discussed [4]. The optimization of the bearing means, to reduce the output of the bearing among the stresses generated due to load and the overall weight of the bearing [5]. Failure analysis of a ball bearing is performed by using different techniques, such as, oil analysis, wear debris analysis, vibration analysis and acoustic emission analysis [6 & 7]. The analysis of elliptical springs is discussed in paper [8]. The present paper deals with the static structural and transient dynamic analysis of a deep groove ball bearing both theoretically and by using ANSYS.

II. STATIC STRUCTURAL ANALYSIS OF A DEEP GROOVE BALL BEARING

A static structural analysis determines the displacements, stresses, strains, and forces in structures or components caused by loads that do not induce significant inertia and damping effects. In the present work Hertz contact stress, principal stresses, Von Mises stress, Deformations, and strains are calculated both theoretically and by using ANSYS.

II.A THEORETICAL CALCULATION FOR STATIC STRUCTURAL ANALYSIS

Hertz was able to obtain the following expression for the pressure within the ellipsoid contact [9].

$$p = p_{max}\left[1 - \left(\frac{x}{b}\right)^2 - \left(\frac{y}{a}\right)^2\right]^{\frac{1}{2}}$$

Where, *a* and*b* are the semi-major and semi-minor axes of the ellipse.
On integrating the pressure over the contact area, the following relation is obtained.

$$p_{max} = \frac{3F}{2\pi ab}$$

Harris has shown that the ellipticity parameter can be used to relate the curvature difference and the elliptic integrals of the first and second kind as follows:

$$J(k) = \left[\frac{2\Im - \varepsilon(1+\Gamma)}{\varepsilon(1-\Gamma)}\right]^{\frac{1}{2}}$$

Where, the elliptic integrals are as follows:

$$\Im = \int_0^{\frac{\pi}{2}}\left[1-\left(1-\frac{1}{k^2}\right)\sin^2\phi\right]^{-\frac{1}{2}}d\phi,$$

$$\varepsilon = \int_0^{\frac{\pi}{2}}\left[1-\left(1-\frac{1}{k^2}\right)\sin^2\phi\right]^{\frac{1}{2}}d\phi$$

Coefficient in equation for locus of contacting points is given by the following relation:

$$A = \frac{1}{2}\left(\frac{1}{R_1}-\frac{1}{R_2}\right)\text{ mm}^{-1}, B = \frac{1}{2}\left(\frac{1}{R_1}+\frac{1}{R_3}\right)\text{ mm}^{-1}$$

Where, R_1 is the radius of the ball, R_2 is the radius of the inner race groove, and R_3 is the radius of the inner race.

The relation for the constants γ and K are as following:

$$\gamma = \frac{1-v_1^2}{E_1}+\frac{1-v_2^2}{E_2}\text{ MPa}^{-1}, K = \frac{1}{\frac{2}{R_1}-\frac{1}{R_2}+\frac{1}{R_3}}\text{ mm}$$

Where, v_1, v_2 are the poisons ratio of the two surfaces in contact, and E_1, E_2 are the Young's modulii of the two materials in contact.

The relation for the constants n_a and n_b are as following:

$$n_a = \frac{1}{k}\left(\frac{2\times k\times\varepsilon}{\pi}\right)^{\frac{1}{3}}, n_b = \left(\frac{2\times k\times\varepsilon}{\pi}\right)^{\frac{1}{3}}$$

The semi major axis is obtained by the following relation:

$$a = 1.145\times n_a\times(F\times K\times\gamma)^{\frac{1}{3}}\text{ mm}$$

The semi minor axis is obtained by the following relation:

$$b = 1.145\times n_b\times(F\times K\times\gamma)^{\frac{1}{3}}\text{ mm}$$

The maximum contact pressure at the center of the elliptical contact area is:

$$P = \frac{3F}{2\pi ab}\text{ MPa}$$

The maximum deformation is obtained by the following relation:

$$\delta = 1.04\times(F\gamma)^{\frac{2}{3}}\times A^{\frac{1}{3}}$$

The relations for the three principal stresses are as follows:

$$\sigma_1 = \sigma_x = -2v\,p_{\max}\left[\sqrt{\frac{z^2}{a^2}+1}-\left|\frac{z}{a}\right|\right]\text{ MPa}$$

$$\sigma_2 = \sigma_y = -p_{\max}\left[\left(2-\left(\frac{z^2}{a^2}+1\right)^{-1}\right)\sqrt{\frac{z^2}{a^2}+1}-2\left|\frac{z}{a}\right|\right]\text{ MPa}$$

$$\sigma_3 = \sigma_z = -p_{\max}\left(\frac{z^2}{a^2}+1\right)^{-1}\text{ MPa}$$

Where, z is the depth of contact surface.
The maximum shear stress is as follows:

$$\tau_{\max} = \left|\frac{\sigma_1-\sigma_3}{2}\right|$$

The Von Mises stress is obtained as follows:

$$\sigma_{VM} = \sqrt{\left\{\begin{array}{c}\sigma_1^2+\sigma_2^2+\sigma_3^2-\sigma_1\sigma_2-\sigma_2\sigma_3-\sigma_3\sigma_1\\+3\left(\tau_1^2+\tau_2^2+\tau_3^2\right)\end{array}\right\}}$$

Calculate the equivalent strain is as follows:

$$\in = \frac{\sigma}{(2/\gamma)}$$

II.B. STATIC STRUCTURAL ANALYSIS USING ANSYS

A deep groove ball bearing consists of four main elements namely outer ring, inner ring, balls or rolling elements, and the cage or the retainer as shown in Figure 1. The 6200 deep groove ball bearing is modeled in CATIA as per the standard dimensions. The geometry is imported into ANSYS and finely messed as shown in Figure 2. Apply the boundary conditions by fixing the outer ring of the bearing and cylindrical motion between the balls and the outer ring and the balls and the inner ring. The displacement of the inner ring with respect to the shaft is arrested and the static structural analysis is performed for different applied radial loads of 1000 N, 2000 N, 3000 N, 4000 N, and 5000 N respectively. The values of the Von Mises stresses, equivalent strains, deformations, and Contact pressures are obtained for the different radial loads for the four bearings considered.
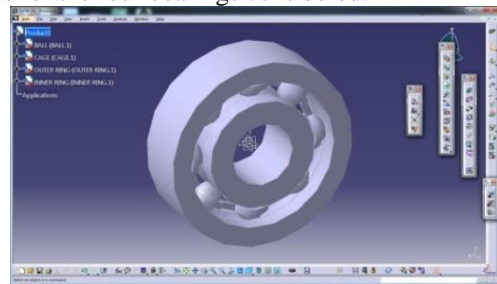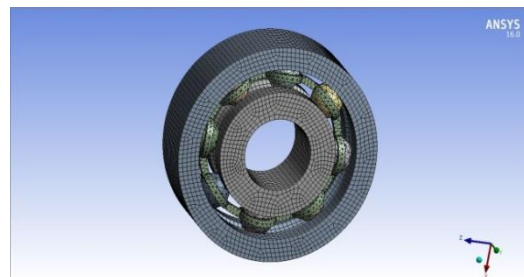
Figure 1 Geometric model of the bearing

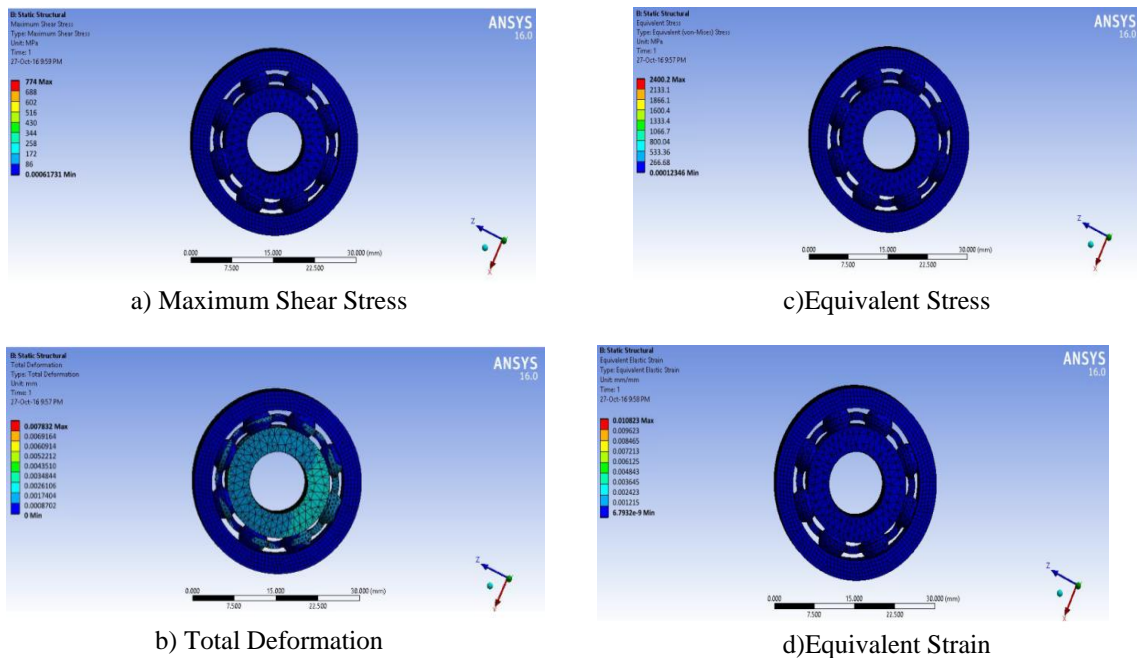Figure 2 Meshing of the bearing

a) Maximum Shear Stress

c)Equivalent Stress

b) Total Deformation

d)Equivalent Strain

Figure 3Static structural analysis results of Stainless Steel bearing

II.C. COMPARISON OF STATIC STRUTURAL ANALYSIS RESULTS

The maximum shear stresses, deformations, Von Mises stresses, and strains obtained from theoretical calculations and static structural analysis using ANSYS for varying loads of 1000 N, 2000 N, 3000 N, 4000 N, and 5000 N for the four bearings considered are tabulated in the Tables 1, 2, 3, and 4 respectively.

Table 1 Comparison of Shear Stresses

Load (N)		Shear Stresses (MPa)			
		Steel	Al_2O_3	ZrO_2	Complete Al_2O_3
1000	Theoretical	758.62	736.84	683.18	979.29
	ANSYS	774.0	753.6	698.1	1000.6
2000	Theoretical	958.53	932.14	864.41	1237.11
	ANSYS	981.8	955.6	886.4	1266.5
3000	Theoretical	1099.54	1070.01	992.50	1419.99
	ANSYS	1100.7	1022.8	1462.3	1100.7
4000	Theoretical	1212.63	1179.77	1094.63	1565.28
	ANSYS	1220.0	1131.6	1617.5	1220.0
5000	Theoretical	1308.09	1273.15	1180.69	1688.73
	ANSYS	1316.1	1227.3	1752.3	1316.1

Table 2 Comparison of Deformations

Load (N)		Deformations (mm)			
		Steel	Al_2O_3	ZrO_2	Complete Al_2O_3
1000	Theoretical	0.0077	0.0063	0.0072	0.0050
	ANSYS	0.0078	0.0064	0.0073	0.0053
2000	Theoretical	0.0123	0.0100	0.0114	0.0087
	ANSYS	0.0124	0.0102	0.0116	0.0091
3000	Theoretical	0.0161	0.0131	0.0150	0.0117
	ANSYS	0.0163	0.0133	0.0152	0.0121
4000	Theoretical	0.0195	0.0159	0.0181	0.0149
	ANSYS	0.0197	0.0162	0.0184	0.0153
5000	Theoretical	0.0226	0.0185	0.0210	0.0171
	ANSYS	0.0230	0.0188	0.0214	0.0175

Table 3 Comparison of Von Mises Stresses

Load (N)		Von Mises Stresses (MPa)			
		Steel	Al_2O_3	ZrO_2	Complete Al_2O_3
1000	Theoretical	2352.49	2277.94	2113.29	3032.52
	ANSYS	2400.2	2329.6	2159.2	3098.6
2000	Theoretical	2958.36	2865.28	2657.44	3816.45
	ANSYS	3029.6	2937.2	2724.3	3907.2
3000	Theoretical	3382.02	3276.39	3038.09	4363.98
	ANSYS	3471.9	3368.4	3130.5	4493.6
4000	Theoretical	3717.68	3603.76	3340.95	4800.31
	ANSYS	3820.6	3726.7	3453.1	4960.7
5000	Theoretical	4001.37	3879.56	3597.03	5167.96
	ANSYS	4125.2	4010.3	3738.9	5361.5

Table 4 Comparison of Equivalent Strains

Load (N)		Equivalent Strains (mm/mm)			
		Steel	Al_2O_3	ZrO_2	Complete Al_2O_3
1000	Theoretical	0.0105	0.0076	0.0085	0.0065
	ANSYS	0.0108	0.0077	0.0087	0.0067
2000	Theoretical	0.0133	0.0095	0.0107	0.0082
	ANSYS	0.0136	0.0098	0.0110	0.0084
3000	Theoretical	0.0152	0.0109	0.0123	0.0094
	ANSYS	0.0156	0.0112	0.0126	0.0097
4000	Theoretical	0.0167	0.0120	0.0135	0.0104
	ANSYS	0.0171	0.0124	0.0139	0.0107
5000	Theoretical	0.0179	0.0129	0.0145	0.0112
	ANSYS	0.0185	0.0133	0.0151	0.0116

## III. TRANSIENT DYNAMIC ANALYSIS OF A DEEP GROOVE BALL BEARING

In, the present work, transient dynamic analysis of the bearing are carried out under the application of load of 1000 N. Transient dynamic analysis gives an overall view of the deformation and stress variation for a period of 10 s upon impact loading of 1000 N at the end of 2 s.

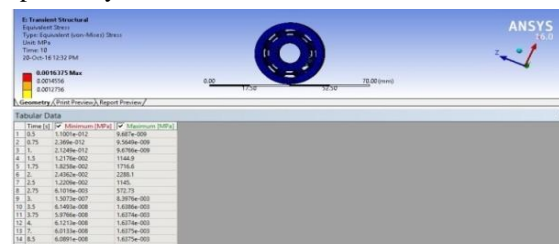### III.A TRANSIENT DYNAMIC ANALYSIS USING ANSYS

Import the IGES file and then select the outer and inner rings and select the material as steel. Select all the balls and select the material zirconium oxide. Select the cage and specify it as yellow brass. Mesh the bearing. Fix the outer ring by selecting the corresponding constraint. Set the number of steps

equal to 5. Set the end times as 1, 2, 3, 4, and 10 s respectively. Apply the force of 1000 N in the Z direction at the end of 2 s and set the force at the remaining seconds to zero. Define the 5 steps by selecting the "Substeps" type. Set the initial substeps to be 2, minimum substeps to be 2, and the maximum substeps to be 3.

The variation in the deformation and Equivalent stresses with respect to time for Deep groove bearing with Zirconium oxide balls for a transient load of 1000 N at the end of 2 s are as shown in the Figures 5.37 and 5.38 respectively. The variation in the deformation and Equivalent stresses with respect to time for Stainless steel, Al_2O_3, ZrO_2, and complete Al_2O_3 bearing for a transient load of 1000 N at the end of 2 s are as shown in the Figures 4, 5, 6 and 7 respectively.
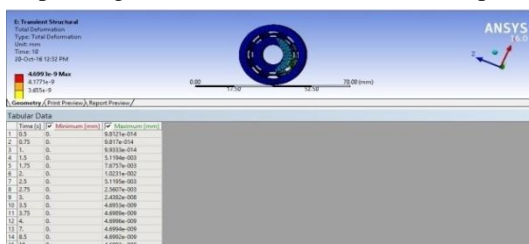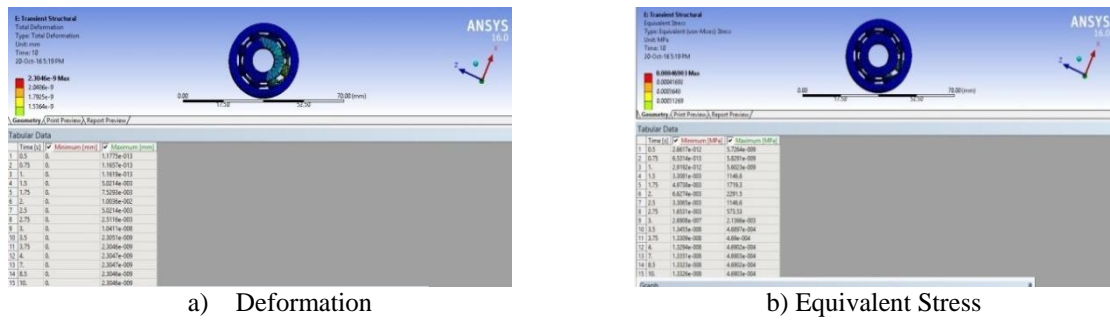

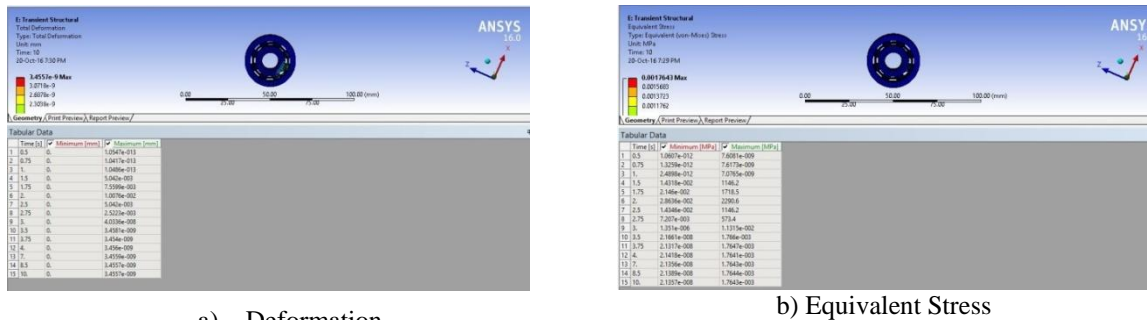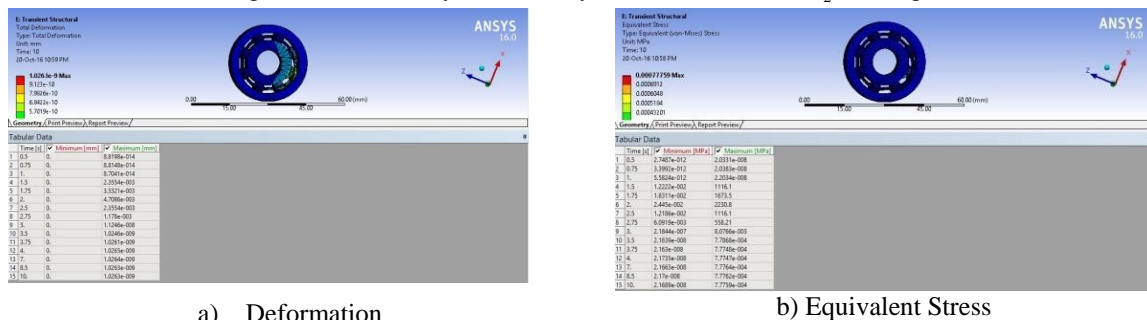a) Deformation   b) Equivalent Stress

Figure 4 Transient Dynamic Analysis Results of Steel bearing

a) Deformation   b) Equivalent Stress

Figure 5Transient Dynamic Analysis Resultsof the Al_2O_3 bearing

a) Deformation   b) Equivalent Stress

Figure 6Transient Dynamic Analysis Resultsof the ZrO_2 bearing

a) Deformation   b) Equivalent Stress

Figure 7Transient Dynamic Analysis Results of complete Al_2O_3 bearing

IV. RESULTS AND DISCUSSIONS

The results obtained from the static structural analysis and Vibrational analysis for all the four bearing materials used for 6200 deep groove ball bearing are discussed in this section.

IV.A COMPARISON OF STATIC STRUCTURAL ANALYSIS RESULTS

Static structural analysis is performed on the 6200 bearing with different materials both theoretically and by using ANSYS. Shear stress, Von Mises-stresses, deformations, and equivalent strains are obtained both theoretically and by using ANSYS. From the values obtained the following conclusions are drawn:

IV.A.1 COMPARISON OF CONTACT PRESSURES

The Contact Pressure at the center of contact surfaces at different applied radial loads in the four types of bearing are as shown in the Figure 8. From the graph, it is clear that deep groove ball bearing completely made up of Aluminum oxide has higher contact stress for the same loading. Complete Steel deep groove ball bearing has relatively lower contact pressure when compared to ceramic and hybrid bearings. Hybrid bearings with steel outer and inner rings, and balls made up of zirconium oxide and aluminum oxide have slightly higher contact pressure when compared to complete steel deep groove ball bearing.
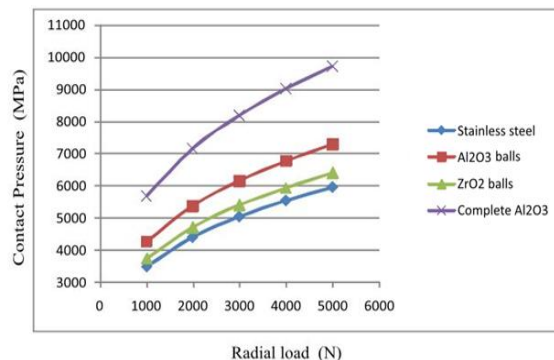

Figure 8 Contact pressure versus Radial Load plot

IV.A.2 COMPARISON OF MAXIMUM SHEAR STRESSES

The Maximum shear stresses for different applied radial loads in the four types of bearing are as shown in the Figure 9. From the graph, it is clear that deep groove ball bearing completely made up of Aluminum oxide has higher maximum shear stress for the same loading. Complete Steel deep groove ball bearing has relatively lower shear stress when compared to ceramic and hybrid bearings. Hybrid bearings with steel outer and inner rings, and balls made up of zirconium oxide and aluminum oxide have slightly higher shear stress when compared to complete steel deep groove ball bearing.
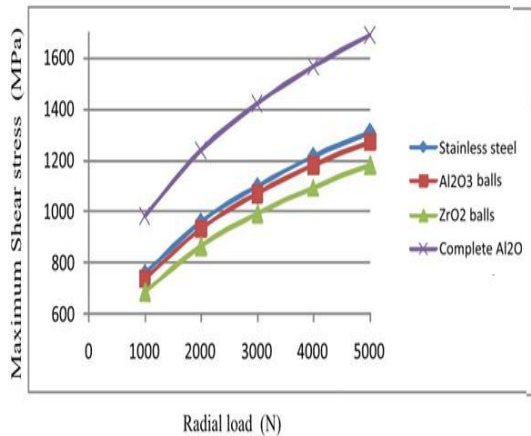

Figure 9 Maximum Shear stress versus Radial Load

IV.A.3 COMPARISON OF DEFORMATIONS

The deformations for different applied radial loads in the four types of bearing are as shown in the Figure 10. From the graph, it is clear that deep groove ball bearing completely made up of Aluminum oxide has lowest deformation for the same loading. Complete Steel deep groove ball bearing has higher deformation when compared to ceramic and hybrid bearings. Hybrid bearings with steel outer and inner rings, and balls made up of zirconium oxide and aluminum oxide have slightly lower shear stress when compared to complete steel deep groove ball bearing.
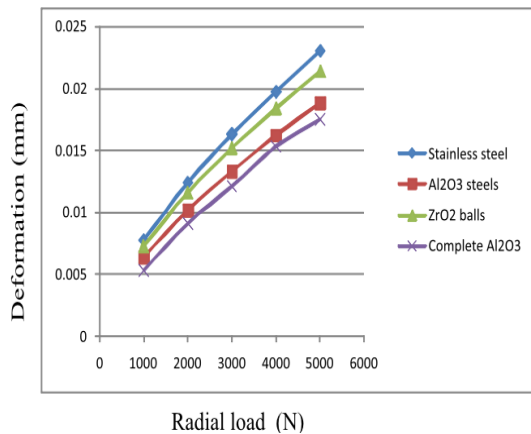

Figure 10 Deformation versus Radial Load

IV.A.4 COMPARISON OF EQUIVALENT (VON-MISES) STRESSES

The equivalent Von Mises stresses for different applied radial loads in the four types of bearing are as shown in the Figure 11. From the graph, it is clear that deep groove ball bearing completely made up of Aluminum oxide has higher maximum equivalent (Von-Mises) stress for the same loading. Complete Steel deep groove ball bearing has relatively lower equivalent stress when compared to ceramic and hybrid bearings. Hybrid bearings with steel outer and inner rings, and balls made up of zirconium oxide and aluminum oxide have slightly higher equivalent stress when compared to complete steel deep groove ball bearing.
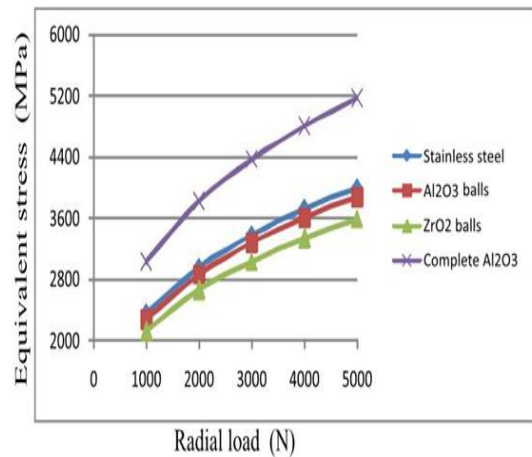

Figure 11 Equivalent (Von-Mises) Stress versus Radial Load

IV.A.5 COMPARISON OF EQUIVALENT STRAINS

The equivalent strains for different applied radial loads in the four types of bearing are as shown in the Figure 12. From the graph, it is clear that deep groove ball bearing completely made up of Aluminum oxide has lowest equivalent strain for the same loading. Complete Steel deep groove ball bearing has higher strain when compared to ceramic and hybrid bearings. Hybrid bearings with steel outer and inner rings, and balls made up of zirconium oxide and aluminum oxide have slightly lower strains when compared to complete steel deep groove ball bearing.
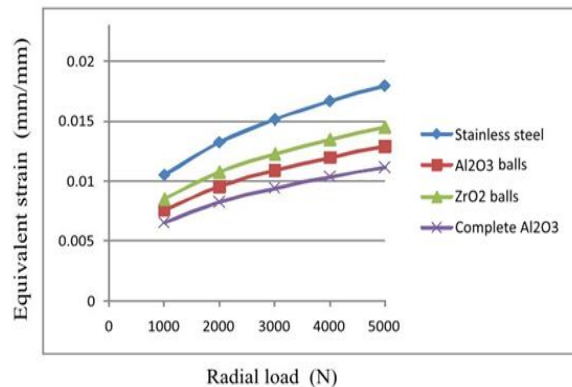

Figure 12 Equivalent Strains versus Radial Load

IV.B COMPARISON OF TRANSIENT DYNAMIC ANALYSIS RESULTS

The stresses obtained at 2 seconds in transient dynamic loading are in coordination with the stresses obtained in static structural analysis. The deformations and equivalent stresses obtained at the end of 2 s in transient dynamic loading and those obtained from static structural analysis are as shown in the Table 5.

Table 5 Comparison of Equivalent Strains

Load (N)		Deformation (mm)			
		Steel	Al_2O_3	ZrO_2	Complete Al_2O_3
1000	Transient	0.0078	0.0075	0.0075	0.0054
	Static Structural	0.0077	0.0063	0.0072	0.0050

V. CONCLUSIONS

Thus, from the results obtained, the ceramic deep groove ball bearings have higher load bearing capacity, lesser tendency for deformation due to wear and friction, The impact load bearing capacity of the ceramic ball bearings are comparatively higher when compared to the hybrid and steel bearings.

The following conclusions are drawn from the project work:

- The theoretical and ANSYS (static structural analysis) results obtained for contact stresses, deformations, Von Mises stresses, and equivalent strains from are in agreement with each other.
- The deformations and stresses obtained from transient dynamic analysis are in agreement with the results obtained from static structural analysis.

References

[1] TANG Zhaopinga and SUN Jianpingb, "The Contact Analysis for Deep Groove Ball Bearing Based on ANSYS", Procedia engineering, 23, pp 423–428, 2011.

[2] R. Pandiyarajan, M.S. Starvin, and K.C. Ganesh, "Contact Stress Distribution of Large Diameter Ball Bearing Using Hertzian Elliptical Contact Theory", Procedia Engineering Volume 38, Pages 264-269, 2012.

[3] Ayao E. Azianou1, Karl Debray, FabriceBolaers, Philippe Chiozzi, Frederic Palleschi, "Modeling of the Behavior of a Deep Groove Ball Bearing in Its Housing," Journal of Applied Mathematics and Physics, Vol. 1, pp-45-50, 2013.

[4] YujuanXu, Mamtimin•Geni, RahmatjanImin, and Bo Lu, "Optimization of Deep Groove Ball Bearing," Contact Interface Parameters and Strength Evaluation, Jeju, Korea, 2013.

[5] RajnikantNagarbhaiAnjara and Milan J Pandya, "Weight Optimization of Deep Groove Ball Bearing", International Journal on Recent and Innovation Trends in Computing and Communication, Vol. 2, pp- 973 – 976, 2014.

[6] Dipen S. Shah and Vinod N. Patel, "A Review of Dynamic Modeling and Fault Identifications Methods for Rolling Element Bearing" Elsevier, Vol. 14, pp 447-456, 2014

[7] AttelManjunath, "D V Girish, "Defect Detection in Deep Groove Polymer Ball Bearing Using Vibration Analysis," International Journal of Recent Advances in Mechanical Engineering , Vol.2, August 2013.

[8] Putti SrinivasaRao, RevuVenkatesh, "Static and Transient Analyses of Leaf Spring Using Composite Material," IUP Journal of Mechanical Engineering Vol 9, 2016.

[9] Putti SrinivasaRao, NadipalliSriraj, and Mohammad Farookh, "Contact Stress Analysis of Spur Gear for Different Materials using ANSYS and Hertz Equation," International Journal of Modern Studies in Mechanical Engineering (IJMSME) Vol 1, pp 45-52, 2015.